

Crystal structure of the bacterial cell division regulator MinD

Suzanne C. Cordell*, Jan Löwe

MRC Laboratory of Molecular Biology, Hills Road, Cambridge CB2 2QH, UK

Received 26 January 2001; revised 7 February 2001; accepted 7 February 2001

First published online 23 February 2001

Edited by Hans Eklund

Abstract In bacterial cell division MinD plays a pivotal role, selecting the mid-cell over other sites. With MinC, MinD forms a non-specific inhibitor of division, that interacts with FtsZ. Specificity is provided by MinD's interaction with MinE at the mid-cell. We have solved the crystal structure of MinD-1 from *Archaeoglobus fulgidus* to 2.6 Å by multiple anomalous dispersion. MinD is a classic nucleotide binding protein, related to nitrogenase iron proteins, which have a fold of a seven-stranded parallel β -sheet, surrounded by α -helices. Although MinD, unlike the proteins it interacts with and those it is structurally related to, is a monomer, not a dimer. © 2001 Federation of European Biochemical Societies. Published by Elsevier Science B.V. All rights reserved.

Key words: Cell division; Crystal structure; MinD; MinC; FtsZ

1. Introduction

When bacterial cells divide a septum forms at the middle, leading to constriction of the cell to form two daughter cells (recent reviews [1–3]). The earliest component of the septum is the tubulin homologue, FtsZ, which forms a ring at the mid-cell. Other proteins, including FtsA and ZipA, are recruited to enable division to progress. It has been suggested that these form a complex, the divisome. To enable successful cell division the mid-cell site must be selected for septum formation and other potential division sites blocked. In *Escherichia coli* this requires MinC, MinD and MinE [4]. MinD interacts with both MinC and MinE [5].

MinD binds to MinC to inhibit cell division, probably by affecting FtsZ [6,7]. Overexpression of MinC in Δ minD cells suppresses the Δ minD phenotype. Hence it is thought that MinD activates MinC by recruiting it to the membrane, increasing the effective local concentration. At the mid-cell MinE forms an annular structure, in Δ minD cells the ring does not form, suggesting MinD also recruits MinE to the membrane [8]. MinE has two domains, the C-terminal one provides topological specificity, though how it selects the mid-cell is uncertain. The N-terminal domain (residues 2–22) interacts with MinD. It is thought that this relieves MinCD induced inhibition at the mid-cell by dissociating the MinCD complex [5], enabling division to occur at the mid-cell, rather than other sites.

In *E. coli* MinD has been found to oscillate from cell pole

to cell pole [9]. MinC also oscillates but this behaviour requires MinD [10]. It has been proposed that this masks potential division sites. Mutagenesis of the ATP binding site to remove ATPase function prevents MinD activating MinC dependent inhibition of cell division [11].

MinD is a peripheral membrane ATPase [11], which is part of a larger family of ATPases. These include the Par proteins, involved in plasmid segregation and nitrogenase iron proteins [12]. After FtsZ, MinD is the most highly conserved component of cell division. It has been found in most eubacteria, archaea and in chloroplasts though not in mitochondria. Here we present the crystal structure at 2.6 Å of MinD-1 from *Archaeoglobus fulgidus*.

2. Materials and methods

2.1. Protein expression and purification

MinD-1 (www.tigr.org) from *A. fulgidus* (DSMZ no. 4304) was cloned into pHis17. C41(DE3) cells were transformed and grown overnight. A single colony was used to inoculate a 5 ml culture of 2 \times TY, 1% glucose and 100 μ g/ml ampicillin and grown for 4 h. The culture was used to inoculate 1 l of 2 \times TY, which was induced with 1 mM IPTG when OD₆₀₀ = 1.0 and the temperature reduced to 25°C. The cells were harvested after 15 h and stored at –70°C.

Cells were lysed and after centrifugation the lysate was applied to a Ni-NTA silica column (Qiagen). Buffer A was 50 mM Tris pH 7.0 and 300 mM NaCl. Buffer B was 50 mM Tris and 1 M imidazole pH 7.0. The column was washed with 5% buffer B and the protein eluted with 40% buffer B. The protein was loaded directly onto a Sephacryl S200 column (Amersham-Pharmacia) equilibrated in 200 mM NaCl, 20 mM Tris, 1 mM EDTA and 1 mM NaN₃ pH 7.0. The protein eluted as a single peak and could be stored at 4°C for several months.

2.2. Seleno-methionine substituted MinD

The seleno-methionine substituted protein was grown in the non-methionine auxotrophic C41(DE3) cells used for the native protein, by a previously described method [13]. The protein was purified as for the native but with the addition of 5 mM β -mercaptoethanol for the Ni-NTA column and 5 mM DTT for the Sephacryl S200 column. Electrospray mass spectroscopy was used to check SeMet incorporation. (Native MinD: observed 28 491.47 Da, calculated 28 622.56 Da; SeMet: observed 28 725.01 Da, calculated 28 903.24 Da, indicating the N-terminal methionine is not present as the difference between calculated and observed values is \sim 149 Da.)

2.3. Crystallisation and data collection

Native crystals were grown using the sitting drop vapour diffusion technique using 2% PEG 6000 and 0.1 M Tris pH 8.6 as the crystallisation solution. Drops composed of 1 μ l protein at 5 mg/ml and 1 μ l crystallisation solution were equilibrated for 3–5 months at 19°C. The crystals were frozen in mother liquor plus 25% PEG 400, belong to space group P4₃2₁2 and have cell dimensions of $a=b=90.31$ Å and $c=83.33$ Å. Seleno-methionine substituted crystals were grown in the same manner as for the native protein but with 9% PEG 2000, and 0.1 M Tris pH 8.0 for the crystallisation solution. Drops were composed of 2 μ l protein at 5 mg/ml and 1 μ l crystallisation solution and equilibrated for 2–3 months at 19°C. A multiple anomalous dispersion

*Corresponding author. Fax: (44)-1223-213556.
E-mail: scc23@mrc-lmb.cam.ac.uk

Table 1
Crystallographic data

Crystal	λ (Å)	Resol. (Å)	I/σ^2	R_m^b (%)	Multipl. ^c	Compl. (%) ^d
PEAK	0.9790	3.2	6.3	0.090	13.2 (6.6)	99.7
INFL	0.9792	3.2	6.4	0.088	15.0 (7.5)	99.6
HREM	0.9393	3.2	6.1	0.084	13.4 (6.7)	99.3
NATI	0.9393	2.6	5.5	0.071	3.3	96.7

Space group $P4_32_12$ (89), $a=b=90.32$ Å, $c=83.33$ Å.

^aSignal to noise ratio for the highest resolution shell of intensities.

^b $R_m = \sum_i |\Sigma_j I(h,i) - I(h)| / \Sigma_i \Sigma_j I(h,i)$ where $I(h,i)$ are symmetry related intensities and $I(h)$ is the mean intensity of the reflection with unique index h .

^cMultiplicity for unique reflections, anomalous multiplicity in brackets.

^dCompleteness for unique reflections, anomalous completeness is identical because inverse beam geometry was used. Correlation coefficients of anomalous differences at different wavelengths for the MAD experiment: PEAK versus INFL: 0.28, PEAK versus HREM: 0.23, INFL versus HREM: 0.14.

(MAD) dataset and the native dataset were collected at ID14-4 ESRF, Grenoble, France. Crystals were indexed and integrated using the MOSFLM package [14] and further processed using the CCP4 package [15].

2.4. Structure determination

An initial 3.2 Å electron density map was generated by locating four selenium sites in the datasets PEAK, INFL and HREM using SOLVE [16] (Table 1). Initial phases were calculated using SOLVE and RESOLVE [17] was used for solvent flattening. Model building was done using MAIN [18] and refinement using the CNS package [19]. The final parameters of the model are summarised in Table 2.

3. Results

Structurally MinD closely resembles other nucleotide binding proteins such as nitrogenase iron proteins and GTPases such as Ffh (PDB entry 1NG1 [20]), part of the signal recognition particle (Figs. 1 and 3). Sequence alignments of MinD and nitrogenase iron proteins indicated MinD would resemble nitrogenases. The amino acid sequence identity between MinD-1 and the nitrogenase from *Clostridium pasteurianum* is 25.5%. The core of MinD is a twisted arch of stacked β -strands, surrounded by α -helices (Fig. 1). The β -sheet arrangement follows that of the nitrogenase iron protein from *C. pasteurianum* (PDB entry 1CP2 [21]), with one antiparallel and seven parallel β -strands in the order 3a-4p-2p-5p-1p-6p-7p-8p. The α -helices are clustered on either side of the stack of β -sheet. On the outside of the arch are helices H2–H6, within the centre of the arch are helices H1, H1', H7, H7', H8.

Table 2
Refinement statistics

Model	Residues 1–233 and 27 water molecules
Diffraction data	NATI, 2.6 Å, all data
R -factor, R -free ^a	0.2058, 0.2251
B average/bonded ^b	52.14 Å ² , 4.754 Å ²
Geometry bonds/angles ^c	0.006 Å/1.332°
Ramachandran ^d	92.4%/0.0%
PDB ID ^e	1HYQ, 1HYQSF

^a5% of reflections were randomly selected for determination of the free R -factor, prior to any refinement.

^bTemperature factors averaged for all atoms and RMS deviation of temperature factors between bonded atoms.

^cRMS deviations from ideal geometry for bond lengths and restraint angles [31].

^dPercentage of residues in the 'most favoured region' of the Ramachandran plot and percentage of outliers [32].

^eProtein Data Bank identifiers for coordinates and structure factors, respectively.

There was no electron density for residues 234–263. The secondary structure prediction suggests a loop of glycine and lysine rich nature followed by an α -helix at the C-terminus.

MinD is an ATPase, containing a P-loop and switch I and II sites, though this structure does not contain nucleotide. The structure of the nitrogenase from *C. pasteurianum* does not contain nucleotide though there is a nitrogenase structure from *Azotobacter vinelandii* containing ADP.AIF₄⁻ (PDB entry 1N2C, [22]), which has been used in this comparison. The P-loop is between strand S1 and helix H1 and the sequence is GKGGTGKTT (Fig. 2). The consensus sequence is GXGGXGK[TS] for a range of proteins similar to MinD. Residues in the P-loop usually bind the α - and β -phosphates

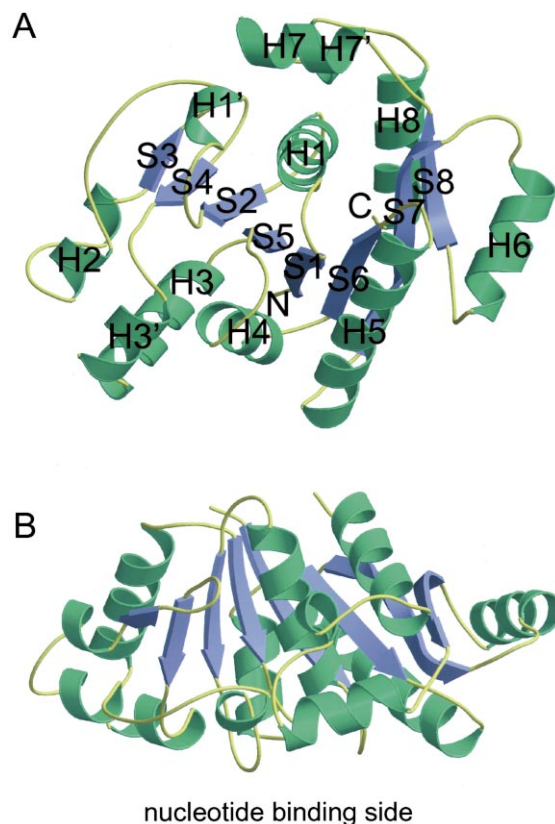
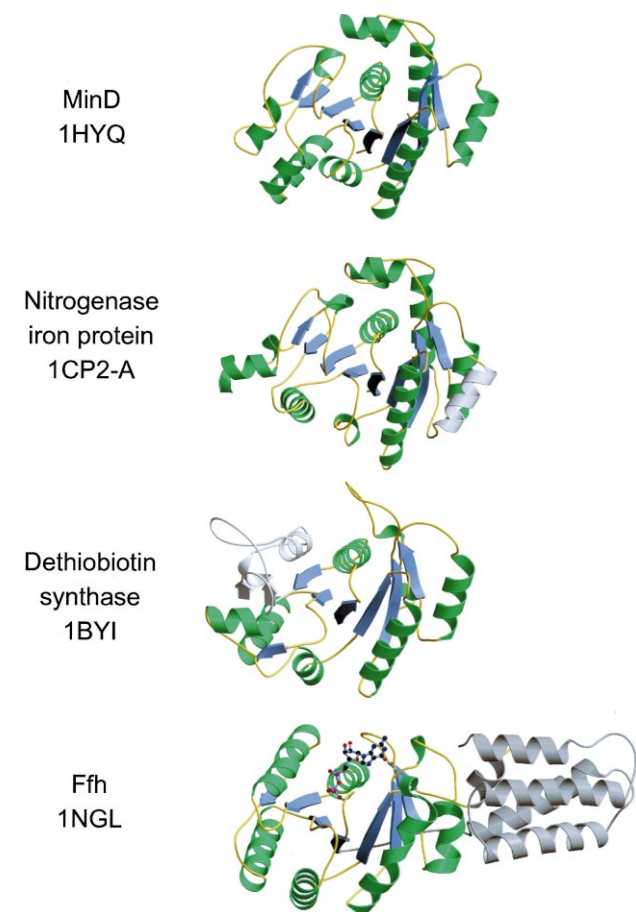


Fig. 1. Ribbon drawings of MinD. A: MinD showing the secondary structure elements, B is rotated 90° around the y axis so the top of the structure in A is now at the front, to show the nucleotide binding face. Made with MOLSCRIPT [33] and RASTER3D [34].



4. Discussion

The MinD crystal structure was solved by multiple anomalous dispersion to 2.6 Å resolution. MinD is part of a large family of nucleotide binding proteins that share a common core fold. MinD is a ‘minimalist’ member of the family as it

Fig. 3. Structural alignment of MinD and structurally similar proteins, in the same orientation as Fig. 1A. Aligned regions are coloured, all others are grey. The nitrogenase iron protein [21] has a Z-score of 25.1 and a root mean square deviation of superimposed C α of 2.6 Å over 223 equivalent residues. For dethiobiotin synthase [24], Z=14.8, with a RMS deviation of superimposed C α of 3.1 Å over 182 equivalent residues. For arsentine translocating ATPase fragment [25], Z=13.7, with a RMS deviation of superimposed C α of 2.9 Å over 178 equivalent residues and for signal sequence recognition protein Ffh fragment [20], Z=12.9 with a RMS deviation of superimposed C α of 2.7 Å over 167 equivalent residues. Made with DALI [23], MOLSCRIPT [33] and RASTER3D [34].

has almost no deviations from the shared fold. Most other proteins it is related to have functionally significant insertions, such as the insertion box in Ffh. How MinD achieves its multiple tasks, of MinC and MinE binding without additional regions is enigmatic.

We have been unable to obtain a MinD structure with nucleotide bound. Residues presumed to be involved in nucleotide binding are involved in the crystal contacts. The predicted switch regions are all on the same surface of the protein, along with the P-loop, at the edge of a shallow indentation that is capped by helix H5 from another molecule in the crystal packing. For the nitrogenase iron protein, from *C. pasteurianum*, an overlap between the dimer interface and the nucleotide binding site was found.

The role of ATP binding and hydrolysis in MinD is not known. Mutations of the P-loop to inhibit ATP hydrolysis have been reported to inhibit MinD induced activation of MinC [11]. This seems at odds with the theory that MinD activates MinC by sequestering it to the membrane, increasing the effective local concentration. The switch II region differs considerably between the nitrogenase and MinD. This is unsurprising as this region is usually the effector in nucleotide binding proteins and the biological function of MinD and the nitrogenase iron protein differ considerably.

MinD has been found to be located at the membrane and is

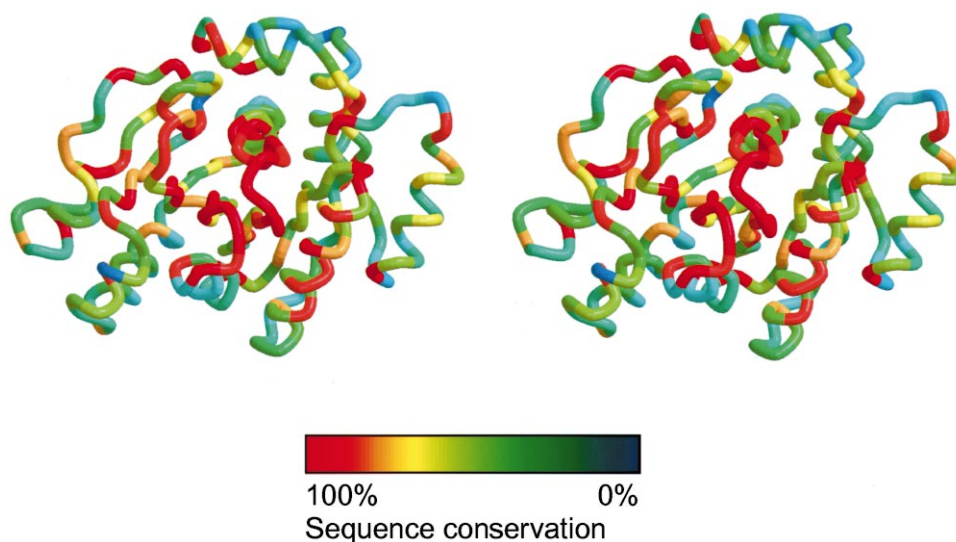


Fig. 4. Stereo drawing of MinD, in the same orientation as Fig. 1A, colour coded according to sequence conservation. 11 MinD sequences from *A. fulgidus*, *E. coli*, *Neisseria meningitidis*, *Vibrio cholerae*, *X. fastidiosus*, *Bacillus subtilis*, *D. radiodurans*, *Helicobacter pylori*, *Synechocystis* sp., *A. aeolicus* and *Thermotoga maritima* were aligned. Organisms other than *A. fulgidus* contain both MinC and MinD. The degree of sequence identity is shown as colours between red and blue. 100% sequence conservation corresponds to red. Made with MOLSCRIPT [33] and RASTER3D [34].

essential for MinE ring formation and MinC activation [8,11], indicating that MinD is involved in recruiting these proteins to the membrane. We can find no structural evidence that MinD binds to the membrane directly, suggesting that MinD binds to another protein that is located at the membrane. The identity of a potential MinD receptor is unknown, though discovery of such a protein would facilitate understanding of the system that locates the middle of the bacterium prior to septum formation.

MinD is the last of the three Min proteins to have its structure solved (Cordell, S.C., Anderson, R. and Löwe, J., unpublished results) [27]. As it is the only one to interact with the other two it is now possible to discuss potential sites of interaction between the proteins. Residues 2–22 of MinE are necessary and sufficient to inhibit MinCD activity. NMR studies of this region indicate a nascent helix, where there is rapid interconversion between disordered and α -helical conformations. This helix could be stabilised on interaction with MinD, potentially forming a heterodimeric coiled coil [28]. As all the helices in MinD are at the surface, any could be the interaction site with MinE. One potential candidate is the predicted C-terminal helix of MinD. There is no electron density for this region, or the preceding glycine lysine rich loop, indicating the region is flexible. In *E. coli* mutation of G263D produces a minicell phenotype [29]. The glycine residue is conserved in the alignment of MinD and is preceded by two lysines in the consensus sequence.

MinD is known to bind the C-terminal domain of MinC (*E. coli* 116–231), with no reported interactions to the N-terminal domain [30]. The C-terminal domain is a β -helix, with one of the three faces involved in dimerisation to another β -helix (Cordell, S.C., Anderson, R. and Löwe, J., unpublished results). This surface is hydrophobic so it is unlikely that MinD disrupts the dimer when binding nor does it seem plausible that MinE dissociates the MinCD complex via separation of the MinC dimer. This leaves the two hydrophilic surfaces of the β -helix free to bind MinD, of these surface C has been proposed to interact with MinD as it contains a charged region. In *E. coli* mutation of MinC G176R affects MinCD interaction [5], though the MinC structure indicates this mutation is on the C-face but is structural rather than functional, as it occurs at the end of a strand in the β -helix.

The nucleotide binding surface of MinD is the only region with a high level of sequence conservation, mostly due to nucleotide binding requirements. This seems a likely site for interaction with another protein as the conserved region extends beyond the nucleotide binding site. One idea is that binding to another protein, such as MinC or MinE, promotes ATP hydrolysis. Many of the proteins structurally similar to MinD bind other proteins affecting nucleotide hydrolysis. For the nitrogenase iron protein ATP is not hydrolysed unless it is bound to the Fe-Mo protein. For Ffh, GTP is not hydrolysed unless it is bound to FtsY. The ArsA ATPase is slightly different as heavy metal ion binding increases the rate of hydrolysis.

MinD, unlike the proteins it interacts with and those it is structurally similar to, is monomeric. This is surprising, especially as the ATPase sites are split across monomers or domains. The nitrogenase dimer has the two active sites split across each monomer. Residues supplied by the first subunit and involved in nucleotide hydrolysis are conserved in the MinD (*A. vinelandii* numbers with MinD numbers in brackets). These are the P-loop, Asp-36 (40) from switch I and the

Asp-125 (117) from switch II, though the Ser-16 residue in the P-loop that is hydrogen bonded to Asp-125 and also coordinates the Mg^{2+} is a Thr (17) in the MinD alignment. The residues provided by the second subunit appear to be conserved in the MinD. Lys-10 (11) is found in all the MinD aligned, Asp-129 though is not. Instead there is a Glu residue (123) in the same region that could play a functionally similar role.

We hypothesise that at some point during MinD's interactions with MinC, MinE and nucleotide MinD dimerises and that this regulates a biologically significant step in bacterial cell division. One possibility is that MinD could be like p21 (ras) which requires an exchange protein to affect nucleotide exchange. Because MinD is structurally similar to nitrogenase, a mechanism where dimerisation promotes nucleotide exchange seems more favourable. This could be MinC, MinE or the hypothetical membrane protein that locates MinD and so MinC and MinE to the membrane.

Acknowledgements: We thank Gordon Leonard at beamline ID14-4, ESRF (Grenoble) for assistance with MAD data collection and Sew Peak-Chew (MRC-LMB, Cambridge) and Ian Fearnley (MRC Dunn Nutrition Unit, Cambridge) for performing mass spectrometry.

References

- [1] Rothfield, L., Justice, S. and Garcia-Lara, J. (1999) *Annu. Rev. Genet.* 33, 423–448.
- [2] de Boer, P.A.J., Cook, W.R. and Rothfield, L.I. (1990) *Annu. Rev. Genet.* 24, 249–274.
- [3] Lutkenhaus, J. and Addinall, S.G. (1997) *Annu. Rev. Biochem.* 66, 93–116.
- [4] de Boer, P.A.J., Crossley, R.E. and Rothfield, L.I. (1989) *Cell* 56, 641–649.
- [5] Huang, J., Cao, C. and Lutkenhaus, J. (1996) *J. Bacteriol.* 178, 5080–5085.
- [6] Hu, Z.L., Mukherjee, A., Pichoff, S. and Lutkenhaus, J. (1999) *Proc. Natl. Acad. Sci. USA* 96, 14819–14824.
- [7] Justice, S.S., Garcia-Lara, J. and Rothfield, L.I. (2000) *Mol. Microbiol.* 37, 410–423.
- [8] Raskin, D.M. and de Boer, P.A.J. (1997) *Cell* 91, 685–694.
- [9] Raskin, D.M. and de Boer, P.A.J. (1999) *Proc. Natl. Acad. Sci. USA* 96, 4971–4976.
- [10] Raskin, D.M. and de Boer, P.A.J. (1999) *J. Bacteriol.* 181, 6419–6424.
- [11] de Boer, P.A.J., Crossley, R.E., Hand, A.R. and Rothfield, L.I. (1991) *EMBO J.* 10, 4371–4380.
- [12] Koonin, E.V. (1993) *J. Mol. Biol.* 229, 1165–1174.
- [13] Van Duyn, G.D., Standaert, R.F., Karplus, P.A., Schreiber, S.L. and Clardy, J. (1993) *J. Mol. Biol.* 229, 105–124.
- [14] Leslie, A.G.W. (1991) in: *CCP4 and ESF-EACMB Newsletters on Protein Crystallography*, SERC Laboratory, Daresbury.
- [15] Coll. Comput. Project, N. (1994) *Acta Crystallogr.* D50, 760–763.
- [16] Terwilliger, T.C. and Berendzen, J. (1999) *Acta Crystallogr. Sect. D Biol. Crystallogr.* 55, 849–861.
- [17] Terwilliger, T.C. (2000) *Acta Crystallogr. Sect. D Biol. Crystallogr.* 56, 965–972.
- [18] Turk, D. (1992) Ph. D. Thesis, Technische Universität München.
- [19] Brunger, A.T. et al. (1998) *Acta Crystallogr. Sect. D Biol. Crystallogr.* 54, 905–921.
- [20] Freymann, D.M., Keenan, R.J., Stroud, R.M. and Walter, P. (1997) *Nature* 385, 361–364.
- [21] Schlessman, J.L., Woo, D., Joshua-Tor, L., Howard, J.B. and Rees, D.C. (1998) *J. Mol. Biol.* 280, 669–685.
- [22] Schindelin, N., Kisker, C., Schlessman, J.L., Howard, J.B. and Rees, D.C. (1997) *Nature* 387, 370–376.
- [23] Holm, L. and Sander, C. (1995) *Trends Biochem. Sci.* 20, 478–480.
- [24] Huang, W.J., Lindqvist, Y., Schneider, G., Gibson, K.J., Flint, D. and Lorimer, G. (1994) *Structure* 2, 407–414.

- [25] Zhou, T.Q., Radaev, S., Rosen, B.P. and Gatti, D.L. (2000) *EMBO J.* 19, 4838–4845.
- [26] Pichoff, S., Vollrath, B., Touriol, C. and Bouche, J.P. (1995) *Mol. Microbiol.* 18, 321–329.
- [27] King, G.F., Shih, Y.L., Maciejewski, M.W., Bains, N.P.S., Pan, B.L., Rowland, S.L., Mullen, G.P. and Rothfield, L.I. (2000) *Nat. Struct. Biol.* 7, 1013–1017.
- [28] King, G.F., Rowland, S.L., Pan, B., Mackay, J.P., Mullen, G.P. and Rothfield, L.I. (1999) *Mol. Microbiol.* 31, 1161–1169.
- [29] Labie, C., Bouche, F. and Bouche, J.P. (1990) *J. Bacteriol.* 172, 5852–5855.
- [30] Hu, Z.L. and Lutkenhaus, J. (2000) *J. Bacteriol.* 182, 3965–3971.
- [31] Engh, R.A. and Huber, R. (1991) *Acta Crystallogr. Sect. A* 47, 392–400.
- [32] Laskowski, R.A., Macarthur, M.W., Moss, D.S. and Thornton, J.M. (1993) *J. Appl. Crystallogr.* 26, 283–291.
- [33] Kraulis, P.J. (1991) *J. Appl. Crystallogr.* 24, 946–950.
- [34] Merritt, E.A. and Bacon, D.J. (1997) in: *Macromolecular Crystallography, Pt B*, Vol. 277, pp. 505–524.
- [35] Barton, G.J. (1993) *Protein Eng.* 6, 37–40.